

Charged-Hadron Inclusive Cross Sections and Fractions in e^+e^- Annihilation at $\sqrt{s}=29$ GeV

H. Aihara, M. Alston-Garnjost, R. E. Avery, A. Barbaro-Galtieri, A. R. Barker, B. A. Barnett, D. A. Bauer, A. Bay, G. J. Bobbink, C. D. Buchanan, A. Buijs, D. O. Caldwell, H.-Y. Chao, S.-B. Chun, A. R. Clark, G. D. Cowan, D. A. Crane, O. I. Dahl, M. Daoudi, K. A. Derby, J. J. Eastman, P. H. Eberhard, T. K. Edberg, A. M. Eisner, R. Enomoto, F. C. Ern , K. H. Fairfield, J. M. Hauptman, W. Hofmann, J. Hylen, T. Kamae, H. S. Kaye, R. W. Kenney, S. Khacheryan, R. R. Kofler, W. G. J. Langeveld, J. G. Layter, W. T. Lin, F. L. Linde, S. C. Loken, A. Lu, G. R. Lynch, R. J. Madaras, B. D. Magnuson, G. E. Masek, L. G. Mathis, J. A. J. Matthews, S. J. Maxfield, E. S. Miller, W. Moses, D. R. Nygren, P. J. Oddone, H. P. Paar, S. K. Park, D. E. Pellett, M. Pripstein, M. T. Ronan, R. R. Ross, F. R. Rouse, K. A. Schwitkis, J. C. Sens, G. Shapiro, B. C. Shen, J. R. Smith, J. S. Steinman, R. W. Stephens, M. L. Stevenson, D. H. Stork, M. G. Strauss, M. K. Sullivan, T. Takahashi, S. Toutouchi, R. van Tyen, W. Vernon, W. Wagner, E. M. Wang, Y.-X. Wang, W. A. Wenzel, Z. R. Wolf, H. Yamamoto, S. J. Yellin, and C. Zeitlin

(TPC/Two-Gamma Collaboration)

Lawrence Berkeley Laboratory, University of California, Berkeley, California 94720

University of California at Davis, Davis, California 95616

University of California Institute for Research at Particle Accelerators, Stanford, California 94305

University of California at Los Angeles, Los Angeles, California 90024

University of California at Riverside, Riverside, California 92521

University of California at San Diego, San Diego, California 92093

University of California at Santa Barbara, Santa Barbara, California 93106

Carnegie-Mellon University, Pittsburgh, Pennsylvania 15213

Ames Laboratory, Iowa State University, Ames, Iowa 50011

Johns Hopkins University, Baltimore, Maryland 21218

University of Massachusetts, Amherst, Massachusetts 01003

New York University, New York, New York 10003

National Institute for Nuclear and High Energy Physics, Amsterdam, The Netherlands

University of Tokyo, Tokyo, Japan

(Received 9 May 1988)

We report measurements of π^\pm , K^\pm , and p,\bar{p} inclusive cross sections and fractions in e^+e^- annihilation at $\sqrt{s}=29$ GeV, for the momentum interval $0.01 < z = p/p_{\text{beam}} < 0.90$. The analysis is based on approximately 70 pb^{-1} of data collected with the TPC/ 2γ detector facility at the SLAC storage ring PEP. Detector upgrades result in significantly improved momentum coverage and precision of the data, compared to previous measurements.

PACS numbers: 13.65.+i, 13.87.Fh

Inclusive hadron cross sections and charged-hadron fractions in e^+e^- annihilation are fundamental quantities providing information about quark fragmentation. In this paper we present measurements of these quantities with substantially improved accuracy and extending to higher z , where $z \equiv p_{\text{hadron}}/p_{\text{beam}}$, than previously reported.¹⁻⁴ The particle spectra in the high- z region provide a sensitive probe of the hadron production mechanism, especially for the case of baryons. For example, dimensional-counting arguments⁵ predict that the baryon to meson ratio should fall as $(1-z)^1$ or $(1-z)^2$ for $z \rightarrow 1$, whereas the Lund string model,⁶ e.g., predicts a rising baryon fraction. The potential to discriminate between competing hadron production models is enhanced at high z by the fact that a comparatively large fraction of the particles in this region are produced

directly in the hadronization process, rather than as the result of resonance decays.

We have measured the π^\pm , K^\pm , and p,\bar{p} inclusive cross sections and fractions in the interval $0.01 < z < 0.90$ with the TPC/ 2γ detector at the PEP e^+e^- storage ring at SLAC, operating at $\sqrt{s}=29$ GeV. The TPC/ 2γ facility has been described in detail in Ref. 7. The present analysis is based on approximately 70 pb^{-1} of data collected between 1984 and 1986, and uses only charged-particle information from the time projection chamber (TPC) itself. The detector configuration during this period included a 13.25-kG superconducting magnet and a gating-grid system to reduce track distortions, resulting in a momentum resolution of typically $(\Delta p/p)^2 = (1.5\%)^2 + (0.65\% p)^2$ (p in GeV/ c).

Charged particles are identified by a simultaneous

measurement of momentum and ionization energy loss (dE/dx). A charged particle passing through the TPC's gas volume (80% Ar and 20% CH₄ at a pressure of 8.5 atm) produces several hundred ionization electrons per cm. These electrons are detected by multiwire proportional chambers (sectors). Up to 183 dE/dx measurements are obtained for each track. These dE/dx values are corrected for electron capture and diffusion along the drift path, variations in wire gain over the surface of a sector, variations between sectors, polar-angle dependence (resulting from dependence on the length of track sampled by each sense wire), and gain variations due to changes in gas density and composition. The most probable dE/dx is estimated by forming the mean of the lowest 65% of the usable measurements. In the following, this quantity is referred to as the truncated mean dE/dx , or simply the " dE/dx " of a particle. For typical tracks with 120 dE/dx measurements a resolution for the truncated mean dE/dx of approximately 3.5% is obtained.

Much of the momentum range studied in this analysis corresponds to the relativistic-rise region of the dE/dx versus velocity curve. In this region the separation between particle species is at most 3.5 standard deviations. Hence, the particle identity cannot be established on a track-by-track basis and the relative abundances must be determined by a statistical analysis. This procedure requires an accurate knowledge of both the expected dE/dx as a function of the particle's velocity and the dE/dx resolution.

An atomic physics model for ionization energy loss was used to predict the expected dE/dx as a function of the particle's speed.⁷⁻⁹ The model prediction was scaled to fit the average dE/dx measured for samples of well-identified particles, such as protons from the $1/\beta^2$ region, pions from the minimum-ionizing and relativistic-rise regions, cosmic-ray muons, conversion electrons, and Bhabha electrons. The protons, pions, and conversion electrons were taken from multihadron events. The data points and resulting fit are shown in Fig. 1(a). The systematic uncertainty in the dE/dx versus velocity relation is estimated to 0.2% [determined from systematic differences between different data sets, such as pions in hadronic events and cosmic-ray muons; see inset in Fig. 1(a)].

The resolution for the truncated mean, $\sigma_{dE/dx}$, was determined from a sample of approximately 47000 minimum-ionizing pions in multihadron events. The resolution is mainly a function of the number m of usable dE/dx measurements and decreases as $1/\sqrt{m}$, with a floor of about 1.8%. The dE/dx resolution function is Gaussian out to 3 standard deviations [Fig. 1(b)]. Studies with cosmic-ray muons indicate that the relative resolution $\sigma_{dE/dx}/(dE/dx)$ remains approximately independent of the mean dE/dx of the track sample for the relativistic-rise region. For the $1/\beta^2$ region, the relative resolution was observed to improve somewhat with in-

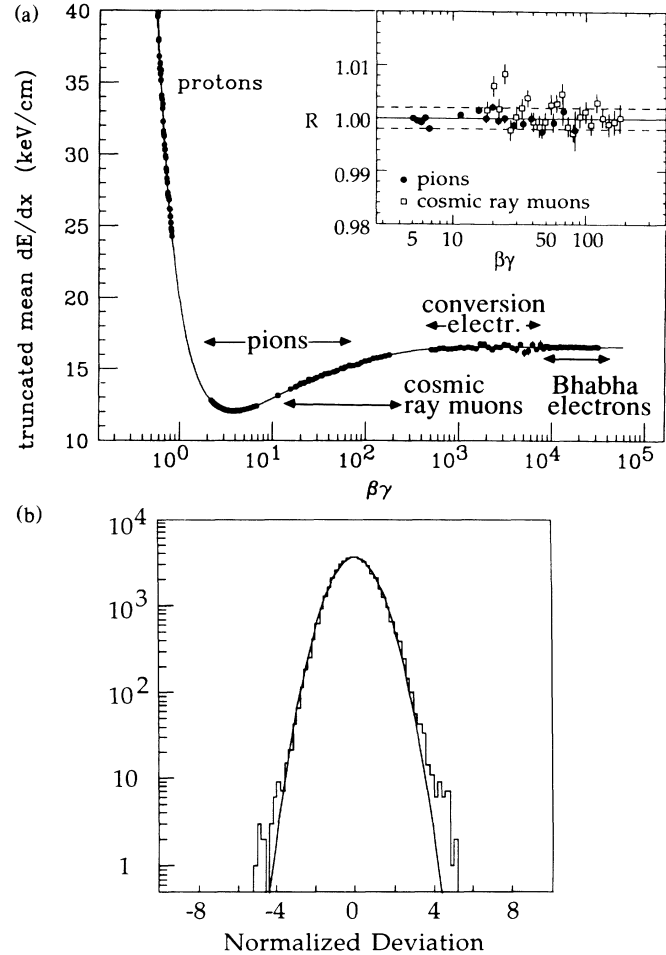


FIG. 1. (a) Average truncated mean dE/dx as a function of $\beta\gamma=p/m$ of a particle, as determined from protons, pions, and conversion electrons in hadronic events, from cosmic-ray muons, and from Bhabha electrons. Line: (adjusted) atomic physics model. Inset: ratio R of data points and model fit in the relativistic-rise region. The dashed lines indicate the 0.2% systematic uncertainty. (b) Distribution in difference between measured and predicted dE/dx for minimum-ionizing pions, normalized to the dE/dx resolution for each track. The curve represents a normal distribution ($\sigma=1$).

creasing mean dE/dx . [Empirically, $\sigma_{dE/dx}/(dE/dx) \propto (dE/dx)^{-0.35}$.] The fractional systematic uncertainty in the dE/dx resolution is estimated to be 8%. A more detailed discussion of the dE/dx analysis can be found in Refs. 7 and 9.

The selection of multihadron events is described in Ref. 3. For this analysis, it was further required that the angle between the sphericity axis and the beam line be larger than 45° , resulting in a final sample of 20126 events. Tracks in these events were required to have at least forty dE/dx measurements for determination of the truncated mean, an error in the measurement of the momentum component transverse to the beam of $\Delta p_T/p_T < 0.15$ or $\Delta p_T/p_T^2 < 0.15 \text{ GeV}^{-1}$, and a polar angle

larger than 30°, and to extrapolate back to within 3 cm of the event vertex in the bend plane and to within 5 cm along the direction of the beam. At low momenta, a substantial fraction of the observed protons come from nuclear interactions in the material between the interaction point and the TPC. Therefore, only negative particles are used for $z < 0.25$.

For determination of the hadron fractions and cross sections, the track sample is divided into narrow momentum intervals. For each interval, the number of particles ϕ_i of each type ($i = e, \pi, K, \text{ and } p$) is determined by an extended maximum-likelihood fit¹⁰ to the dE/dx distribution (Fig. 2). The fit does not require binning in dE/dx and makes maximal use of the information available for each track. The likelihood function is given by

$$L = \exp \left(- \sum_i \phi_i \right) \prod_j \left[\sum_i \frac{\phi_i}{\sqrt{2\pi}\sigma_{ij}} \exp \left(\frac{-[R_j - \mu_i(p_j)]^2}{2\sigma_{ij}^2} \right) \right],$$

where the index j runs over all tracks in the momentum interval, and i runs over the four particle species: electrons, pions, kaons, and protons. R_j is the measured dE/dx for track j divided by the predicted value for a pion at the measured momentum of the track; σ_{ij} is the resolution in R_j for particle hypothesis i , which is estimated from the number of dE/dx measurements, the polar angle, and the curvature error of the track; $\mu_i(p_j)$ is the expected R value for a track of momentum p_j and particle species i . We do not attempt to separate pions from muons, but instead subtract the muon rate obtained in an independent measurement.¹¹

The number of hadrons in each momentum interval was then corrected for effects of geometrical acceptance, nuclear interactions in the material between the interaction point and the TPC, decays in flight, event and track selection cuts, muon contamination of the pion sample, momentum smearing, initial-state radiation, and back-

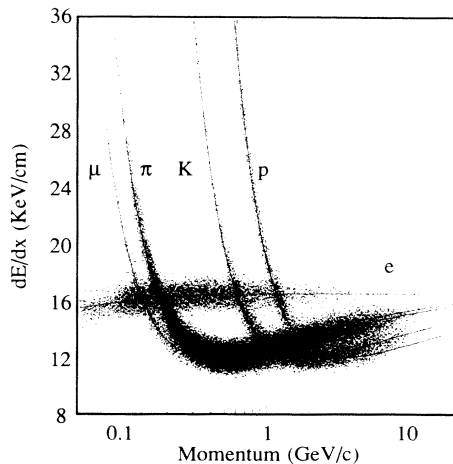


FIG. 2. Distribution in dE/dx vs momentum for particles in multihadron events. Lines indicate the predicted average dE/dx as a function of momentum for different species.

ground from the reactions $e^+e^- \rightarrow \tau^+\tau^-$ and $e^+e^- \rightarrow e^+e^- + \text{hadrons}$. The background corrections are small compared to the estimated errors in the fractions and cross sections. Protons are defined to include decay protons of weakly decaying baryons; pions include decay products of K_S^0 but not those of K_L^0 .

The inclusive cross sections $(1/\sigma\beta)(d\sigma/dx)$, with $x = 2E/\sqrt{s}$ and $\beta = p/E$, are presented in Fig. 3, which also includes previously reported data by Aihara *et al.* (TPC Collaboration)³ and Althoff *et al.* (TASSO Collaboration).⁴ The cross sections are normalized to the total annihilation cross section into hadrons. Figure 4 shows the corresponding hadron fractions as a function of $z \equiv p_{\text{hadron}}/p_{\text{beam}}$. The errors shown in Figs. 3 and 4 correspond to the quadratic sum of systematic and statistical uncertainties. For the cross sections, statistical errors dominate above $z \sim 0.5$. The dominant sources of systematic error for the proton and kaon cross sections come from uncertainty in the dE/dx versus velocity curve and in the relative dE/dx resolution. The systematic error in the pion cross section is dominated by a 2% uncertainty in the pattern-recognition efficiency. For the particle fractions, many of the systematic uncertainties cancel to first order, and errors in the fractions are predominantly statistical.

In confirmation of earlier results,^{3,4} the particle fractions at low z show a steep momentum dependence of the K^\pm and p, \bar{p} content of jets (Fig. 4). Above $z \approx 0.3$, the fractions level off. In particular, the p, \bar{p} fraction remains constant within errors for $z > 0.2$, in contrast with the decreasing baryon fraction predicted by counting rules for $z \rightarrow 1$,⁵ and the rising baryon fraction pre-

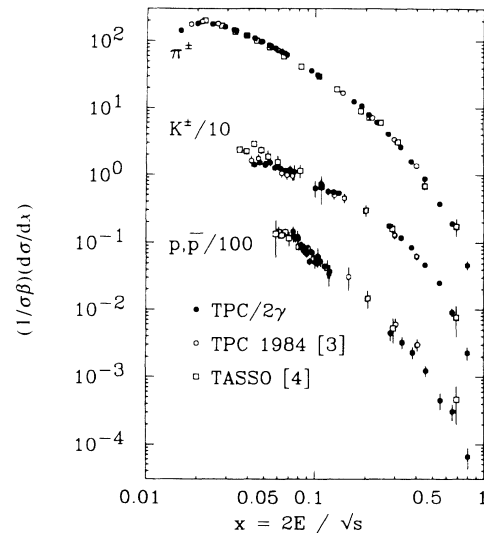


FIG. 3. Normalized cross sections $(1/\sigma\beta)(d\sigma/dx)$ for π^\pm , K^\pm , and p, \bar{p} , as a function of $x = 2E/\sqrt{s}$, including earlier TPC Collaboration (Ref. 3) and TASSO Collaboration (Ref. 4) data.

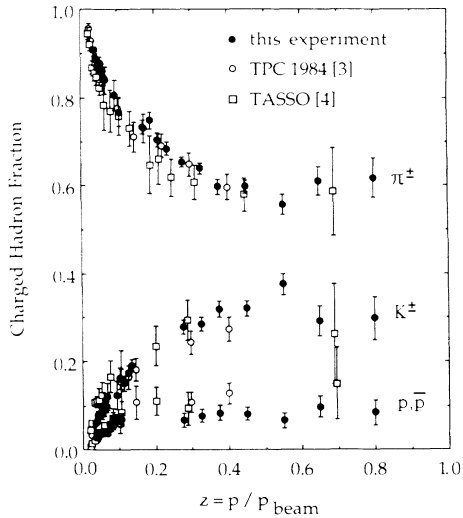


FIG. 4. Fractions of pions, kaons, and protons among charged hadrons in multihadron events, as a function of $z = p/p_{\text{beam}}$. Included are earlier TPC Collaboration (Ref. 3) and TASSO Collaboration (Ref. 4) data.

dicted by typical fragmentation models with a diquark mechanism for baryon production.^{6,12} With use of their default parameters, none of the most commonly used fragmentation models^{6,12,13} is consistent with our data. More details and comparisons with model predictions are given in Ref. 9.

The efforts of the SLAC PEP staff, and the engineers, programmers, and technicians who made this work possible are gratefully acknowledged. This work was supported in part by the U.S. Department of Energy, the Na-

tional Science Foundation, the Joint Japan-U.S. Collaboration in High Energy Physics, and the Foundation for Fundamental Research on Matter in The Netherlands.

¹M. Derrick *et al.* (HRS Collaboration), Phys. Rev. D **35**, 2639 (1987).

²H. Schellman *et al.* (Mark II Collaboration), Phys. Rev. D **31**, 3013 (1985).

³H. Aihara *et al.* (TPC Collaboration), Phys. Rev. Lett. **52**, 577 (1984).

⁴M. Althoff *et al.* (TASSO Collaboration), Z. Phys. C **17**, 5 (1983), and contribution to the International Symposium on Lepton and Photon Interactions at High Energies, Kyoto, Japan, August 1985 (unpublished), paper No. 399.

⁵S. Brodsky and G. Farrar, Phys. Rev. Lett. **31**, 1153 (1973); V. A. Matveev *et al.*, Nuovo Cimento Lett. **1**, 719 (1973); S. Brodsky and J. Gunion, Phys. Rev. D **17**, 848 (1978).

⁶B. Andersson, G. Gustafson, G. Ingelman, and T. Sjöstrand, Phys. Rep. **97**, 31 (1983).

⁷H. Aihara *et al.* (TPC/2 γ Collaboration), LBL Report No. LBL-23737, 1988 (to be published).

⁸W. Allison and J. Cobb, Ann. Rev. Nucl. Part. Sci. **30**, 253 (1980).

⁹G. D. Cowan, Ph.D. thesis, University of California, Berkeley, LBL Report No. LBL-24715, 1988 (unpublished).

¹⁰L. Lyons, *Statistics for Nuclear and Particle Physicists* (Cambridge Univ. Press, Cambridge, 1986), p. 100.

¹¹H. Aihara *et al.* (TPC Collaboration), Phys. Rev. D **31**, 2719 (1985), and Z. Phys. C **27**, 39 (1985).

¹²T. D. Gottschalk and D. A. Morris, Nucl. Phys. **B288**, 927 (1987).

¹³B. R. Webber, Nucl. Phys. **B238**, 492 (1984).

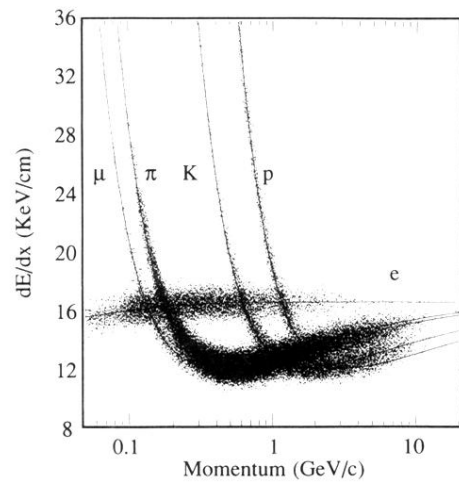


FIG. 2. Distribution in dE/dx vs momentum for particles in multihadron events. Lines indicate the predicted average dE/dx as a function of momentum for different species.